



Impact failure models and application condition of trees in debris-flow hazard mitigation

Ke JIN, Jian-gang CHEN, Xiao-qing CHEN, Wan-yu ZHAO, Guang-wu SI, Xing-long GONG

View online: <https://doi.org/10.1007/s11629-020-6510-8>

Articles you may be interested in

[Quantitative evaluation of eco-geotechnical measures for debris flow mitigation by improved vegetation-erosion model](#)

Journal of Mountain Science. 2022, 19(7): 2015 <https://doi.org/10.1007/s11629-021-7285-2>

[Mitigation measures of debris flow and landslide risk carried out in two mountain areas of North-Eastern Italy](#)

Journal of Mountain Science. 2022, 19(6): 1808 <https://doi.org/10.1007/s11629-021-7212-6>

[Risk assessment of glacial debris flow on alpine highway under climate change: A case study of Aierkuran Gully along Karakoram Highway](#)

Journal of Mountain Science. 2021, 18(6): 1458 <https://doi.org/10.1007/s11629-021-6689-3>

[Comparison of different sampling strategies for debris flow susceptibility mapping: A case study using the centroids of the scarp area, flowing area and accumulation area of debris flow watersheds](#)


Journal of Mountain Science. 2021, 18(6): 1476 <https://doi.org/10.1007/s11629-020-6471-y>


[Effects of loose deposits on debris flow processes in the Aizi Valley, southwest China](#)



Journal of Mountain Science. 2020, 17(1): 156 <https://doi.org/10.1007/s11629-019-5388-9>


Original Article


Impact failure models and application condition of trees in debris-flow hazard mitigation


JIN Ke^{1,3}  <https://orcid.org/0000-0002-8800-9047>; e-mail: jinke@imde.ac.cn

CHEN Jian-gang^{1,2}  <https://orcid.org/0000-0001-6001-5413>; e-mail: chenjg@imde.ac.cn

CHEN Xiao-qing^{1,2,3*}  <https://orcid.org/0000-0002-0177-0811>;  e-mail: xqchen@imde.ac.cn

ZHAO Wan-yu^{1,3}  <https://orcid.org/0000-0003-4879-7541>; e-mail: wyzhao@imde.ac.cn

SI Guang-wu^{1,3}  <https://orcid.org/0000-0001-9952-5250>; e-mail: siguangwu@imde.ac.cn

GONG Xing-long^{1,3}  <https://orcid.org/0000-0003-1311-0420>; e-mail: gongxinglong@imde.ac.cn

*Corresponding author

¹ Key Laboratory of Mountain Hazards and Earth Surface Process, Institute of Mountain Hazards and Environment, Chinese Academy of Sciences, Chengdu 610041, China

² China-Pakistan Joint Research Center on Earth Sciences, CAS-HEC, Islamabad 45320, Pakistan

³ University of Chinese Academy Sciences, Beijing 100049, China

Citation: Jin K, Chen JG, Chen XQ, et al. (2021) Impact failure models and application condition of trees in debris-flow hazard mitigation. *Journal of Mountain Science* 18(7). <https://doi.org/10.1007/s11629-020-6510-8>

© Science Press, Institute of Mountain Hazards and Environment, CAS and Springer-Verlag GmbH Germany, part of Springer Nature 2021

Abstract: Forestry has played an important role in hazard mitigation associated with debris flows. Most forest mitigation measures refer to the experience of soil and water conservation, which disregard the destructive effect of debris flows, causing potentially serious consequences. Determination of the effect of a forest on reducing debris-flow velocity and even stopping debris flows requires distinguishing between when the debris flow will destroy the forest and when the trees will withstand the debris-flow impact force. In this paper, we summarized two impact failure models of a single tree: stem breakage and overturning. The influences of different tree sizes characteristics (stem base diameter, tree weight, and root failure radius) and debris-flow characteristics (density, velocity, flow depth, and boulder diameter) on tree failure were analyzed. The observations

obtained from the model adopted in this study show that trees are more prone to stem breakage than overturning. With an increase in tree size, the ability to resist stem breakage and overturning increases. Debris-flow density influences the critical failure conditions of trees substantially less than the debris-flow velocity, depth, and boulder diameter. The application conditions of forests in debris-flow hazard mitigation were proposed based on the analysis of the model results. The proposed models were applied in the Xijijiehaizi Gully as a case study, and the results explain the destruction of trees in the forest dispersing zone. This work provides references for implementing forest measures for debris-flow hazard mitigation.

Keywords: Trees; Impact failure model; Forest application condition; Debris flow mitigation

Received: 03-Oct-2020
Revised: 10-Jan-2021
Accepted: 05-May-2021

1 Introduction

In mountainous areas, forestry is an important part of bioengineering and has an important role in mitigating debris-flow hazards (Cui et al. 2007; Liu et al. 2017; VanDine 1996). Restoring forest cover can greatly reduce the hazards associated with debris flow by strengthening loose soil (De Baets et al. 2006; Wahren et al. 2012; Vannoppen et al. 2017) and regulating surface concentration flows (Stokes et al. 2014; Wang et al. 2020; Arnone et al. 2016; Ng 2017). In addition, forests can dissipate debris-flow energy, weaken the peak flux, and limit the flow mobility path by presenting a rigid barrier (Booth et al. 2020; Guthrie et al. 2010; Johnson et al. 2000). Forests have been commonly utilized around the world to mitigate debris-flow hazards (Huebl and Fiebiger 2005; Carlados and Piton 2016; Cui et al. 2003; Stokes et al. 2010). Although there have been many successful applications, most current debris-flow forest measures reference the experience of erosion control and disregard the destructiveness of debris flows (Cascini et al. 2020; Cui et al. 2013; Thouret et al. 2020). Improper use of forest may result in tree destruction, which leads to large wood debris in debris flows and thus wood jams (Galia et al. 2018; Piton and Recking 2015; Schmid et al. 2016), which can increase the scale of a subsequent hazard and result in a more serious event. As a consequence, the function of a forest on reducing debris-flow velocity and even stopping debris flows depends on whether the debris flow destroys the forest or the trees withstand the debris-flow impact force. Understanding the critical failure condition of trees can provide specific information about the hazard process (Mitsch 1998; Whelchel et al. 2018).

The main cause of forest damage is additional loading over the tree stem strength, which causes stem breakage, if the bending moment applied exceeds the strength of the root-soil plate, which leads to overturning (Quine and Gardiner 2007). Empirical analysis and mechanical calculations are usually performed to study tree damage. Peltola (1993, 1999) constructed models for the mechanism of windthrow for a single tree, and suggested that trees with a height-to-diameter ratio over a certain threshold were subject to a greater risk of stem breakage and overturning. Dorren (2005a, 2005b) calculated the ability of rockfall to damage trees and the resulting movement path based on experiments, and the results

suggested an exponential relationship between the tree breast height diameter and the maximum amount of energy that tree stem breakage can dissipate. Stokes (2005) measured the spatial position and type of 423 damaged trees caused by rockfall in the French Alps, and discussed the relationship between the damage mode of stem break and occurrence of overturning of different species. Tanaka (2009) conducted an investigation after a flood event, considering that the tree damage mode can be expressed as a function of stem diameter and that severe scour may reduce the threshold of overturning. Tanaka (2011) analyzed the effects of root architecture and physical tree characteristics on tree overturning. Gardiner (2000) developed mathematical models for predicting the critical wind speed and turning moment needed to break the stem and overturn of coniferous trees. Olmedo (2006, 2018) built a model which use discrete element method to analyze the dynamic response of tree stems to rockfall impacts. Many efforts have been made to calculate the damage threshold of trees in other hazards, however, research on the relationship between debris flows and tree damage is still lacking. The results for other hazards may not be directly applied to debris flows due to the complex characteristics of debris flows (Iverson and Denlinger 2001). The dynamic damage mechanism of a tree in debris flows is difficult to quantify because the debris-flow impact distribution and impact force can vary greatly with the change in debris-flow characteristics and boulder size (Hu et al. 2011). Considering such a mechanism is still an effective method for evaluating the impact force of debris flows on a structure in static conditions (Vagnon 2019; Zeng et al. 2014).

In this paper, we summarized the impact failure models of a single tree induced by debris flow, proposed mechanical models for tree breakage failure and overturning failure, and analyzed the important impact factors. We investigated case studies of the mechanical model, and calculated the critical velocity and boulder diameter of the debris flow. The application conditions of forests in debris-flow hazard mitigation were proposed based on the analysis results.

2 Methods

2.1 Impact failure modes of a tree in debris flows

A maintained forest has a persistent role in controlling debris flows. Trees should be able to maintain healthy growth patterns and even endure disturbances caused by debris flows (Polster and Bio. 2002). To better understand the destructive effect of debris flows on trees, we summarized two types of impact failure modes for a single tree based on field investigations and literature inventories. The first failure model is tree stem breakage, which occurs when the debris-flow impact force exceeds the bending strength of a tree stem and then causes damage (Fig. 1a, 1b and 1d). The second failure mode is tree overturning, which occurs when the debris-flow impact force exceeds the anchoring capacity of the roots systems (Fig. 1c and 1d). Presently, the dynamic response of trees to debris-flow impact is still unclear. We applied a static model to analyze the damage of a single tree. We estimate the critical debris-flow velocity and large boulder diameter for different tree sizes and debris-flow depths. The results can help to analyze the application of forests in debris-flow hazard mitigation.

2.2 Debris-flow impact models

The debris-flow impact force can be divided into the static pressure force, dynamic pressure force, and impact force of a large boulder collision (Poudyal et al. 2019). A tree can be assumed to be a cylinder, considering that debris flows impact trees above ground level. The static pressure force can be assumed to be zero when considering a cylindrical tree. According to the balance of momentum and impulse principle for estimating impact force, a hydraulic model is adopted to calculate the debris-flow dynamic pressure (Hung et al. 1984; Moos et al. 2018; Zhang 1993; Vagnon 2019).

$$P_m = \alpha \times \rho_d \times v^2 \times \sin \theta \quad (1)$$

where α is the empirical pressure coefficient, ρ_d is the debris-flow density, v is the debris-flow velocity, and θ is the angle between the flow direction and the direction normal to the impacting plane.

A considerable amount of literature on boulder collisions in debris flows has been published. These studies mostly focus on boulder collisions against

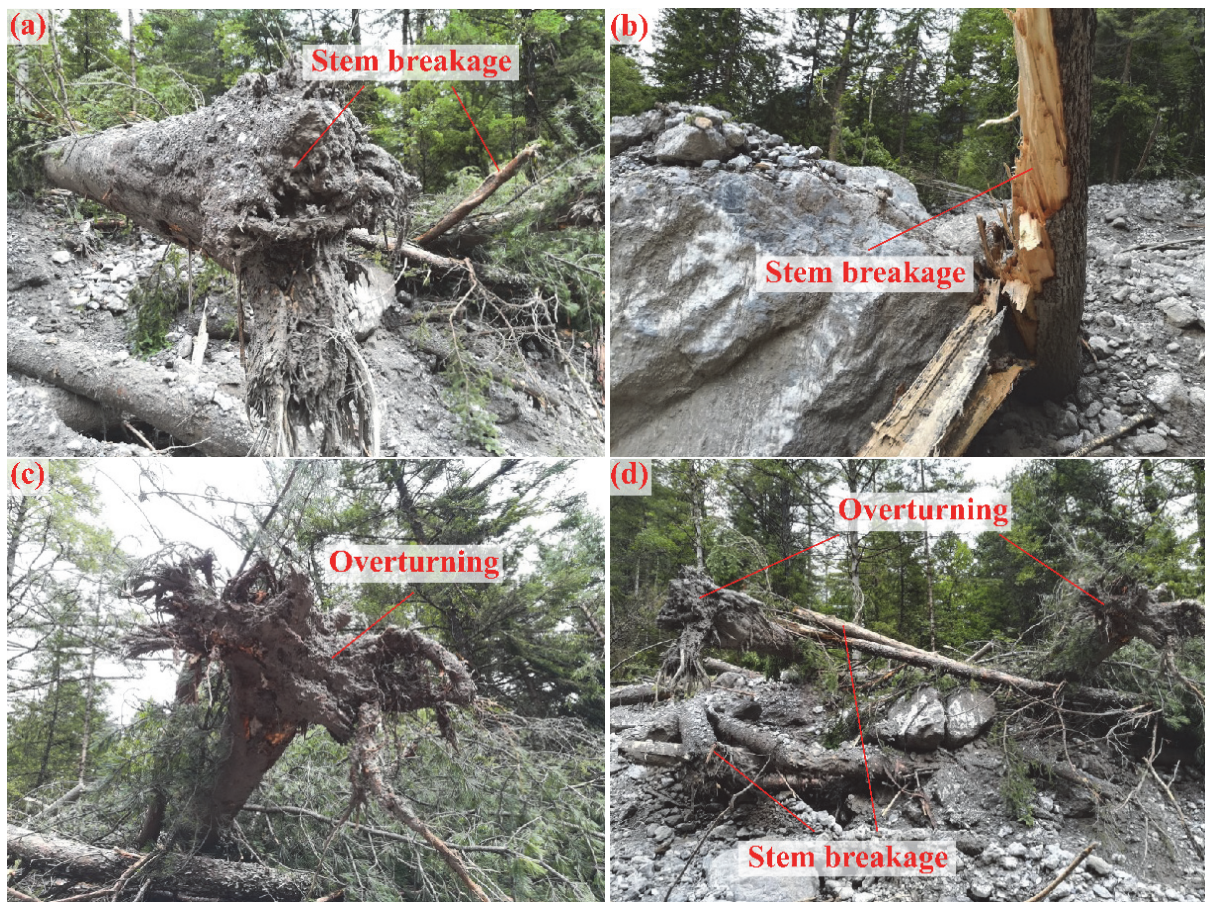


Fig. 1 Trees stem breakage and overturning caused by a debris flow.

rigid structures, such as check dams and bridge piers (Rossi and Armanini 2019; Wang et al. 2018). Derived from the Hertz contact theory, which considers the elastic collision of spherical particles, the impact force of debris flow on a protective structure was deduced, and the corresponding expression was modified via experimental results (He et al. 2016). Most of the results were calculated by assuming the parameters of stone and concrete, which do not apply to trees. A tree, as a biological material, will bend under the action of external forces, and the structural deformation is more important than the contact deformation (Hung and Morgan 1984). Plastic deformation of a tree stem has irreversible effects on the growth of the tree, may cause the tree to lose the ability to hydrologically adjust, may result in the roots systems providing less soil reinforcement, and may even kill the tree. Therefore, this paper considers a tree as a cylindrical cantilever structure and calculates the critical condition of the elastic deformation of a single tree under the action of external forces, the tree bending strain energy (V_ϵ) can be expressed as follows:

$$V_\epsilon = \frac{F_b^2 h^3}{6EI} \quad (2)$$

The boulder kinetic energy (E_k) can be expressed as follows:

$$E_k = \frac{1}{2}mv^2 \quad (3)$$

By equating the tree bending strain energy with the boulder kinetic energy, the boulder impact force F_b can be written as:

$$F_b = \sqrt{\frac{3EImv^2}{h^3}} \quad (4)$$

where E is the bending elastic modulus of the tree stem, I is the area moment of inertia of the stem, v is the debris-flow velocity, and h' is the impact height of the boulder, and m is the mass of the boulder, which can be express as $4\pi r^3\rho_b/3$, where ρ_b is the boulder density. In this paper, it is assumed that the debris-flow velocity is the same as the boulder, and that the diameter of the boulder is equal to the debris-flow depth (Hung and Morgan Kellerhals 1984). The impact height of a large boulder is equal to half of the debris-flow depth, while the destruction of trees is due to the peak impact force of the debris flow and boulders.

2.3 Stem breakage failure model

Tree stem breakage is mainly affected by the stem structure and material properties. The stem tensile strength parallel to the grain is greater than its compressive strength parallel to the grain. A tree stem will break on the side under compression when it is bent. The relationship between the ultimate bending moment of the stem (M_u) and the bending stress of the stem (σ) can be expressed as (Peltola and Kellomäki 1993):

$$M_u = \frac{2I\sigma}{d} \quad (5)$$

where d is the stem base diameter, and I is the area moment of inertia of the stem, and can be expressed as follows:

$$I = \frac{\pi d^4}{64} \quad (6)$$

The schematic diagram of the stem impact by debris flows and boulders is depicted in Fig. 2a. Different from stem breakage in wind or a snow avalanche that external forces will be applied to the crown, which causes the tree weight contributes a lot to the stem to bent (Peltola et al. 1999). Debris flows mainly act at the base of the stem and produce only slight bending. Therefore, disregarding the stem bending influence of the tree weight, tree bending is affected only by the debris flow. The relationship among the bending moment applied by the debris flows (M_d), the boulder impact force (F_b) and the debris-flow dynamic pressure (P_m) can be expressed as

$$M_d = \frac{1}{2}P_m h^2 d + F_b h' \quad (7)$$

where h is the flow depth and h' is the impact height of the boulder. When M_u is equal to M_d , the tree stem is at its failure point. By combining Eqs. (1), (5), (6) and (7), the critical velocity and boulder diameter (D) of the debris flow at the ultimate bending moment of the stem are related by the following expression:

$$\frac{\pi d^3 \sigma}{32} = \frac{1}{2} \alpha \rho_d v^2 \sin \theta h^2 d + \frac{\pi v h' d^2}{8} \sqrt{\frac{\rho_b E D^3}{2 h'^3}} \quad (8)$$

2.4 Tree overturning failure model

Numerous research studies have suggested that

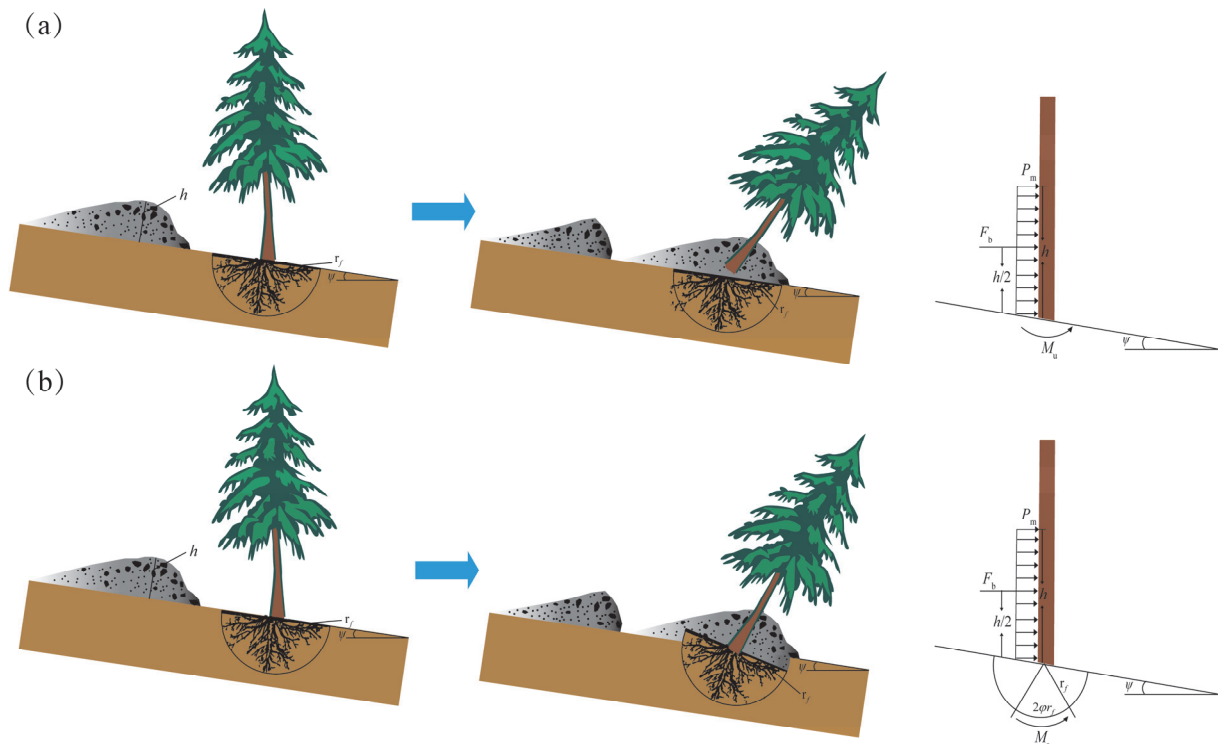


Fig. 2 Schematic illustration of a tree impacted by debris flows with flow depth h on a slope with angle ψ : the corresponding static mechanical model of a single tree is depicted on the right hand side. (a) Stem breakage failure. (b) Overturning failure.

the overturning failure of trees is controlled by the tree species, root spatial distribution, soil friction angle and soil cohesion (Feistl et al. 2015; Moos and Fehlmann 2018; Quine and Gardiner 2007). These factors are complex in the natural environment, which makes them difficult to quantify and analyze. Therefore, this paper refers to the overturning failure model proposed by Bartelt (2001). As shown in Fig. 2b, it is assumed that a lump of soil containing the root cluster and surrounding soil is uprooted when a tree overturn. The main shape of the lump of soil is a half-cylinder with root failure radius r_f and length $2r_f$. The failure surface of the lump of soil lies outside the extent of the root cluster, so the fracturing of the tree roots is disregarded. It is assumed that the weight of the tree disperses with the angle of internal friction and slip length (S_0) is:

$$S_0 = 2\phi r_f \tag{9}$$

where ϕ is the internal friction angle, considering that other parts of the slip surface contribute less, and the main resistance force during overturning is provided by S_0 . The overburden stress that acts on the slip surface is composed of three parts. The first part of the overburden stress arises from the tree weight (σ_t)

(Riley et al. 2019):

$$\sigma_t = \frac{m_t g}{2r_f S_0} \tag{10}$$

where m_t is the tree weight, g is the gravitational acceleration. The second part of the overburden stress arises from the weight of the lump of soil (σ_l). We consider the stress at the center of mass of the lump of soil:

$$\sigma_l = \frac{4r_f}{3\pi} \rho_s g \cos \psi \tag{11}$$

where ψ is the slope angle, and ρ_s is the soil density. The third part of the overburden stress arises from the debris-flow depth (σ_d), which also considers the stress at the lump center of mass:

$$\sigma_d = \rho_d h g \cos \psi \tag{12}$$

The mean shear stress on the slip surface (τ) is:

$$\tau = (\sigma_t + \sigma_l + \sigma_d) \tan \phi + c \tag{13}$$

where c is the soil cohesion. Therefore, the total anti-overturning moment on the slip surface (M_s) is:

$$M_s = 2r_f^2 S_0 \tau \tag{14}$$

By combining Eqs. (7), (9), (13) and (14), the critical velocity and boulder diameter of the debris flow can be calculated when the ultimate bending moment of the stem (M_u) is equal to the total anti-overturning moment:

$$\begin{aligned}
 &4r_f^3\varphi c + m_t gr_f \tan \varphi + \frac{16r_f^4}{3\pi} \varphi \rho_s g \cos \psi \tan \varphi \\
 &+ 4r_f^3 \varphi \rho_d hg \cos \psi \tan \varphi \qquad (15) \\
 &= \frac{1}{2} \alpha \rho_d v^2 \sin \theta h^2 d + \frac{\pi v h' d^2}{8} \sqrt{\frac{\rho_b ED^3}{2h^3}}
 \end{aligned}$$

3 Results and Discussions

Damage conditions to trees in a debris flow were affected by not only their size but also the debris-flow characteristics. To calculate and analyze the failure models of trees during debris flow and the application of forest mitigation measures, we investigated the dispersing forest zone at Xiajijiehaizi Gully, Jiuzhaigou Valley, Sichuan Province, China. Trees of different ages and sizes respond differently to debris flows. According to the data obtained from previous research and field investigations, we selected pine, the dominant tree species in the dispersing forest zone, as the prototype to simulate real trees. We built three tree models to investigate the failure modes of trees of different sizes (Bartelt and Stockli 2001; Peltola and Kellomäki 1993; Peltola et al. 1999). The parameters are shown in Table 1. The critical velocity and boulder size were calculated for dilute (1500 kg/m³) and viscous (2000 kg/m³) debris flows. The empirical pressure coefficient α values are inconsistent in different circumstances (He et al. 2016; Poudyal et al. 2019; Wang et al. 2018). In this paper, considering the form factors of the tree, we utilize the α of 1.0 (Poudyal et al. 2019), the boulder density ρ_b of 2400 kg/m³, and the slope angle ψ of 30°. A debris flow event in Xiajijiehaizi Gully on 21 June 2019 was selected to analyze the model.

3.1 Critical debris-flow velocity and boulder diameter for stem breakage

We used Eq. (8) to figure out the critical velocity and boulder diameter of debris flows to initiate tree stem breakage for different tree sizes (models A, B, and C) and flow depths (0.5 m, 1 m, 1.5 m, and 2 m).

The failure curves of the diluted debris flows plot above those of the viscous debris flows (Fig. 3). When there are large boulders in the debris flow, the trend in the failure curve of the viscous debris flow is similar to the failure curve of the dilute debris flow. However, regardless of the changes in tree size and flow depth, the viscous debris flows are more likely to cause stem breakage than the dilute debris flows. Stem breakage is mainly affected by the boulder size when the flow velocity is low and the boulder size is large. When the flow velocity is high and the boulder size is large, stem breakage is mainly controlled by the debris-flow density.

Table 1 Tree characteristics of different tree sizes in three models (Bartelt 2001; Peltola 1993, 1999).

Parameters	A	B	C
Stem base diameter d (m)	0.158	0.208	0.258
Tree weight m_t (kg)	127	282	524
Root failure radius r_f (m)	0.93	1.16	1.38
Modulus of elasticity E (MOE) (MPa)	7000	7000	7000
Modulus of rupture σ (MOR) (MPa)	39	39	39
Soil density ρ_s (kg/m ³)	1500	1500	1500
Internal friction angle φ (°)	30	30	30
Soil cohesion c (kPa)	5	5	5

The stem breakage curves increase with the size of the trees, and the ability of trees to resist stem breakage in debris-flow hazards increase with tree size (Fig. 3). When the debris flows do not contain large boulders, the critical velocity of model A, B, and C is 8.5-9.8 m/s, 11.2-12.8 m/s and 13.8-15.9 m/s, respectively; when the debris flows include the largest boulder size at the same flow depths, the critical velocities are reduced to 1.2-1.9 m/s (Fig. 3a). Additionally, when the debris flows do not contain large boulders, the critical velocities for the flow depths of 0.5 m, 1.5 m, and 2 m are 22.3-25.7 m/s, 7.4-8.6 m/s and 5.6-6.4 m/s, respectively; when the debris flows include the largest boulder size at the same flow depths, the critical velocities are reduced to 0.8-3.1 m/s (Fig. 3b).

3.2 Critical debris-flow velocity and boulder diameter for overturning

We used Eq. (15) to figure out the critical velocity and boulder diameter of debris flows to initiate tree overturning for different tree sizes (models A, B, and C) and different flow depths (0.5 m, 1 m, 1.5 m, and 2 m).

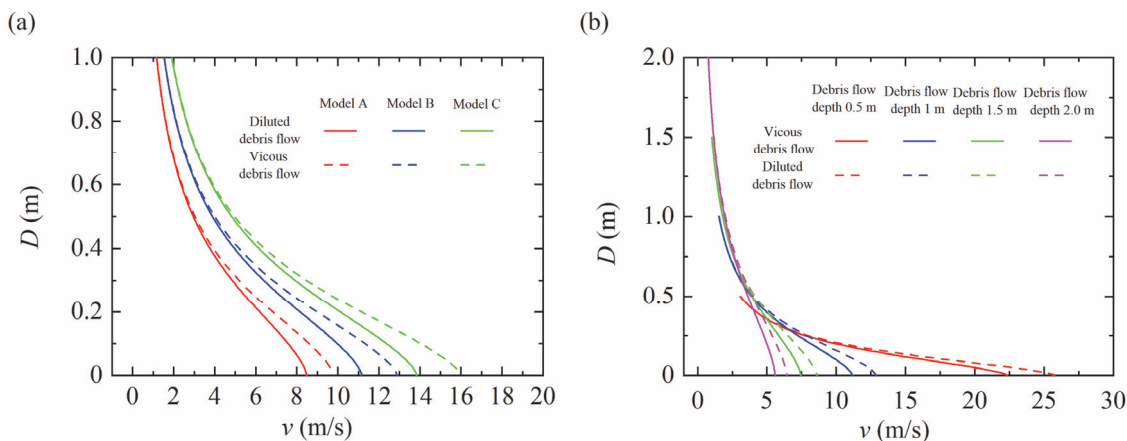


Fig. 3 Critical debris-flow velocity and maximum boulder size for tree stem breakage. (a) Stem breakage in different tree models (flow depth $h=1$ m, models A, B, and C). (b) Stem breakage under different flow depth (model B, flow depth $h=0.5$ m, 1 m, 1.5 m, and 2 m).

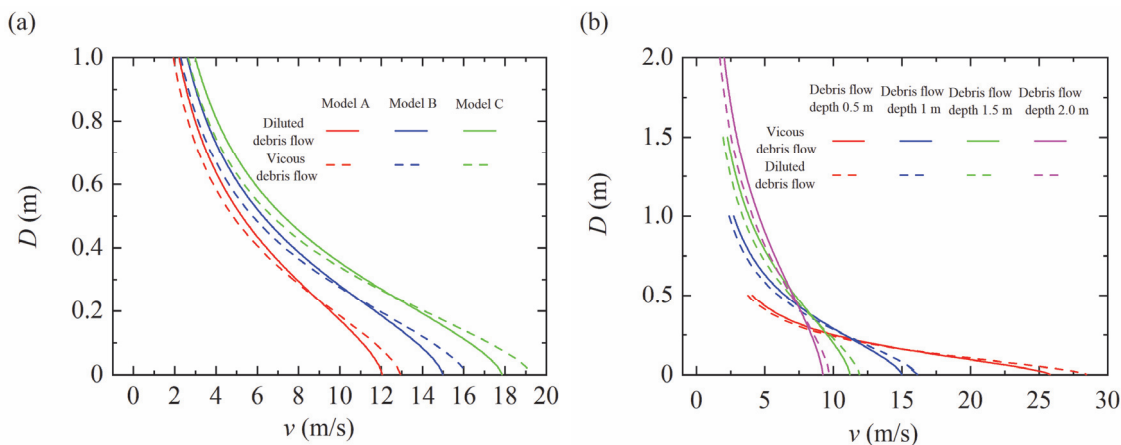


Fig. 4 Critical debris-flow velocity and maximum boulder size for tree overturning. (a) Overturning in different trees model (flow depth $h=1$ m, models A, B, and C). (b) Overturning under different flow depth (model B, flow depth $h=0.5$ m, 1 m, 1.5 m, and 2 m).

Fig. 4 compares the overturning failure curves of the viscous debris flows and the dilute debris flows at a flow depth of 1 m. When the boulder diameter is larger than 0.245 m, the viscous debris-flow damage curves are plotted above the diluted flow damage curves. Or else, the damage curves for the viscous debris flows are plotted below those for the diluted debris flows, which reveals that 0.245 m is the critical particle size when the flow depth is 1 m. If the boulder size is greater than 0.245 m, the cause of overturning is the impact force of the boulder, otherwise, overturning is mainly affected by the dynamic pressure. For different debris-flow depths, the critical boulder diameter increases with the flow depth: the critical boulder diameters are 0.154 m, 0.32 m, and 0.388 m at flow depths of 0.5 m, 1.5 m, and 2 m, respectively.

The overturning curves increase with the size of

the trees, and the ability of trees to resist overturning during debris flows increase with tree size (Fig. 4). When the debris flow does not contain large boulders, the critical velocities of models A, B, and C are 12-12.9 m/s, 14.9-16.1 m/s and 17.8-19.2 m/s, respectively; when the debris flows include the largest boulder size at the same flow depth, the critical velocities are reduced to 2-3.1 m/s (Fig. 4a). When the debris flows do not contain large boulders, the critical velocities for flow depths of 0.5 m, 1.5 m, and 2 m are 25.8-28.4 m/s, 11.2-11.8 m/s and 9.2-9.6 m/s respectively; when the debris flows include the largest boulder size at the same flow depths, the critical velocities are reduced to 1.7-4.1 m/s (Fig. 4b).

3.3 Analysis of application conditions

The calculation and analysis of the impact failure

modes and critical conditions of trees during the debris flows revealed that a tree's anti-destructive ability increases with the stem base diameter. The results show that the stem breakage curves plot below those of the overturning curves, which suggested that trees are more prone to stem breakage than overturning, which is also consistent with previous research (Bartelt and Stockli 2001; Peltola et al. 1999). The failure mode of trees is affected by the debris-flow density, but the debris-flow density is substantially less influential than the flow depth and boulder size.

According to the analysis results of the models, trees can withstand the debris-flow hazard at limited scales. Debris-flow hazards mitigation should fully utilize the hazard mitigation characteristics of both forests and geotechnical engineering. Geotechnical engineering, as a first step toward weakening the magnitude and intensity of debris-flow hazards, will also help to change the debris-flow dynamic conditions that act on a forest, which protects and improves the site conditions of a forest. Forests reduce the occurrence of debris-flow activities via their ecological functions including soil reinforcement (Vergani et al. 2017; Waldron 1976; Waldron and Dakessian 1981), soil erosion resistance (Li et al. 2017; Vannoppen et al. 2015), and hydrology adjustment (Chirico et al. 2013; Vannoppen et al. 2016). Based on our results, the following forest application conditions combined with geotechnical engineering are proposed:

Forest measures such as water conservation forests and slope shelter forests that are utilized to protect slopes, should be matched with diversion dikes and embankments or check dams. The former measures can change the flow path, weaken the debris-flow energy, and reduce velocity and depth of debris flow, and weakens the impact force of the debris flow on the trees to reduce trees failure. The latter measures can raise the erosion datum, intercept solid matter and create more gentle slopes, restrain headward erosion and limit the activation of debris flow substance sources, which is beneficial for tree growth.

Forest measures, such as gully head control forests, gully bank protection forests, and gully bottom dispersing forests, should be matched with geotechnical engineering to intercept solid matter, such as flexible barriers, beam dam, grid dams, silt dams, pile structures, or matched with structures that dissipate energy structures, such as the step-pool dissipation structure. The former measures can

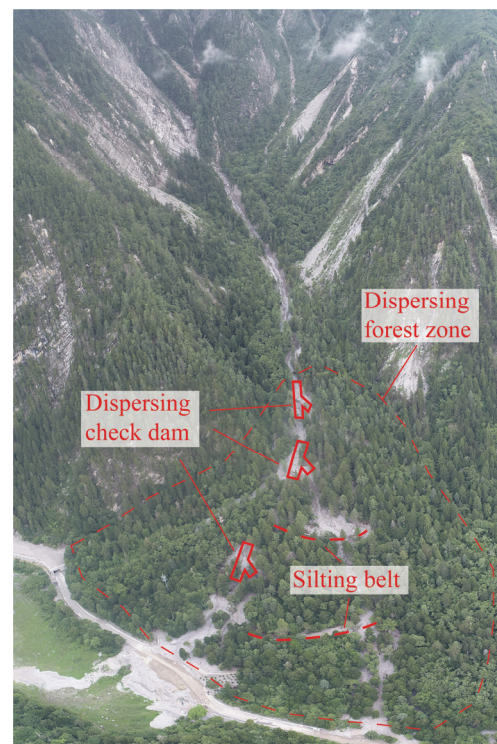


Fig. 5 Full view of Xiajijiehaizi Gully and comprehensive hazard reduction measures.

decrease the solid matter in the debris flow by separating water and particles, which reduces the average particle size and weakens the impact of the debris flow. The latter measures increase the roughness of the gully bed and change the flow pattern, which effectively dissipates the debris-flow energy. Adjusting the flow velocity and flow depth, reduces the severity of the debris flow.

3.4 Application of the models to evaluate debris-flow hazard in Xiajijiehaizi Gully

Xiajijiehaizi Gully, with gully mouth coordinates of $103^{\circ}55'10''$ E, $33^{\circ}07'22''$ N, is located in Jiuzhaigou Valley, Sichuan Province, China. The watershed covers an area of 1.87 km^2 , and the main channel is 2.36 km long. The upstream gully is funnel-shaped, and the gully mouth is a large old debris flow fan on which mixed forest of pine, birch, oak and fir grows. Three dispersing check dams and two silting belts are arranged in the gully, and part of the debris flow channelized enters the dispersing forest zone (Fig. 5).

On 21 June 2019, a destructive debris flow was triggered in Xiajijiehaizi Gully, and the gully mouth after the hazard is shown in Fig. 6a. The flow path was identified, and some trees along the path were

destroyed. Field investigations have shown that both stem breakage and overturning failure occurred, but some trees in the flow path were not damaged. The stem base diameter at the mouth of the Xiajijiehaizi Gully generally ranged from 0.1-0.3 m, as determined during the field investigation, therefore, model A and model C were employed to calculate the critical boulder diameter. The debris-flow density was measured to be 1900 kg/m^3 , with most boulder diameters less than 0.3 m, only a few boulder diameters were greater than 1 m, and the largest boulder diameter was 2.1 m (Fig. 6c). The slope angle of Xiajijiehaizi Gully is 15° . We measured a flow depth of 0.65 m from mud marks on the trees. We calculated the debris-flow velocity to be 3.9 m/s by using the Manning formula in this event (Gong et al. 2020) and substituted the relevant parameters into Eqs. (6) and (12) to calculate the critical boulder diameter. The results show that boulder diameters in the range of 0.37-0.53 m break the tree stems, while boulders with diameters in the range of 0.54 to 0.69 m cause overturning.

It can be seen that the critical size of a boulder that is required to break a tree stem is smaller than that required to overturn a tree. The critical boulder size that is capable of damaging trees is larger than most boulders in debris flows. This finding indicates that trees will not be destroyed when the boulders that come into contact with the trees are not large enough. However, several large boulders that may cause tree failure were transported during this debris flow (Fig. 6c). The failure of a tree is also affected by the probability that it is hit by a large boulder (Fidej et al. 2015; Moos et al. 2018). Wood jams were observed in the dispersing forest zone, which can enhance the impact of debris flows and make trees more vulnerable to destruction (Schmocker and Weitbrecht 2013; Shrestha et al. 2011). Since the properties of natural trees are not as uniform as the model assumes, the defects and differences within trees will also affect the failure mode and corresponding debris-flow critical characteristics (Zhu et al. 2015). These uncertainties also explain why some of the trees on the flow path were damaged, while other trees remained intact. The field investigation indicated that both stem breakage and overturning occurred; however, the models did not consider the effects of root reinforcement and soil water content changes on the properties of the soil, or soil fragmentation disintegration, root abruption or slip out from the soil

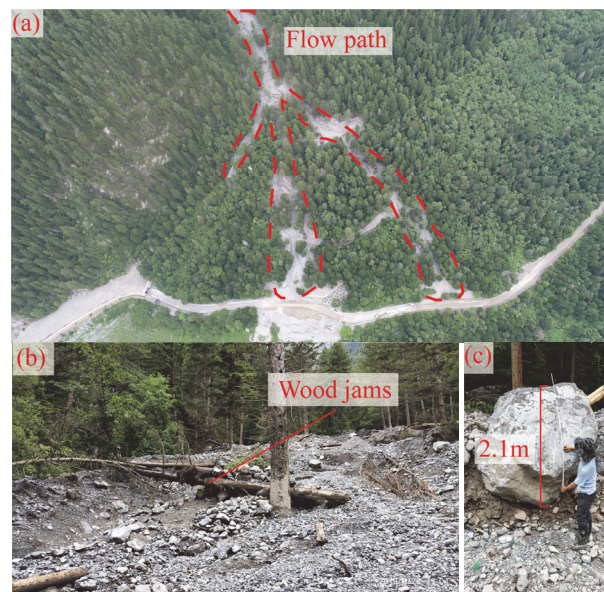


Fig. 6 Images of a Xiajijiehaizi Gully debris flow on 21 June 2019. (a) Debris flow path and isolated trees along the path. (b) Wood jams on the flow path. (c) Large boulder on the flow path.

(Pollen and Natasha 2007). These models may also overestimate the resistance of tree overturning.

The calculated results of the models cannot exactly predict the actual situation, because of the previously mentioned limitations. However, the models can explain the resistance capacity and destruction situation of trees in dispersing forest zones. The limitations of the models can be considered to better enhance the simulation results and computing requirements. This work will further improve our understanding of forest measures to mitigate debris-flow hazards.

4 Conclusion

From information collected during field investigations and the presented model results, we summarized the impact failure models of trees into stem breakage and overturning, and analyzed the failure modes of a single tree in debris flows based on mechanical analysis. The main critical characteristic parameters of debris flow (density, velocity, flow depth, and boulder size) were calculated for the case of tree failure for different tree sizes (stem base diameter, tree weight, and root failure radius). The following observations were made from the models adopted in this study: (1) The change in boulder size,

debris-flow depth, velocity and density can affect the critical failure conditions of trees, while the influence of the debris-flow density is substantially less than that of the boulder size, flow depth and flow velocity. The critical flow velocity decreases rapidly with an increase in flow depth and boulder diameter. (2) Trees are more prone to stem breakage than overturning. With increases in tree size, a tree's ability to resist stem breakage and overturning increases, but tree resistance is limited relative to the destructive power of debris flows. (3) In the process of debris-flow hazard mitigation, implementing appropriate geotechnical engineering measures is most important, because they change the debris-flow dynamic conditions that act on a forest, also, protect and improve the site conditions of the forest by adjusting the boulder size, flow velocity and flow depth. Thus, forests can be effectively and sustainably utilized to take advantage of their ecological function, and reduce the incorporation of large wood in debris flows to prevent more serious events.

Due to the assumptions of the tree's failure conditions and simplifications of debris-flow impact

characteristics made in the calculations, these models present some limitations. However, the models still explain the impact failure of trees in dispersing forest zones, which improves our understanding of sustainable forest bioengineering to mitigate debris-flow hazards. Analyzing and calculating the critical conditions of a single tree failure can provide references for the design of forest measures, in collaboration with geotechnical engineering measures, for debris-flow hazard mitigation.

Acknowledgements

This study is supported by the National Natural Science Foundation of China (Grant No. 41925030), the Strategic Priority Research Program of the Chinese Academy of Sciences (Grant No. XDA23090403), the Youth Innovation Promotion Association of the CAS (Grant No. 2017426), the National Natural Science Foundation of China (Grant No. 51709259), and the CAS "Light of West China" Program.

References

- Arnone E, Caracciolo D, Noto LV, et al. (2016) Modeling the hydrological and mechanical effect of roots on shallow landslides. *Water Resour Res* 52(11): 8590-8612. <https://doi.org/10.1002/2015WR018227>
- Bartelt P, Stockli V (2001) The influence of tree and branch fracture, overturning and debris entrainment on snow avalanche flow. *Ann Glaciol* 32: 209-216. <https://doi.org/10.3189/172756401781819544>
- Booth AM, Sifford C, Vascik B, et al. (2020) Large wood inhibits debris flow runoff in forested southeast Alaska. *Earth Surf Proc Land* <https://doi.org/10.1002/esp.4830>
- Carladous S, Piton G (2016) From the restoration of French mountainous areas to their global management: historical overview of the Water and Forestry Administration actions in public forests. In: 13th Congress INTERPRAEVENT 2016. Lucerne, Switzerland. pp 34-42
- Cascini L, Cuomo S, Pastor M, et al. (2020) Modelling of debris flows and flash floods propagation: a case study from Italian Alps. *Eur J Environ Civ En* 1-24. <https://doi.org/10.1080/19648189.2020.1756418>
- Chirico GB, Borga M, Tarolli P, et al. (2013) Role of vegetation on slope stability under transient unsaturated conditions. *Procedia Environmental Sci* 19: 932-941. <https://doi.org/10.1016/j.proenv.2013.06.103>
- Cui P, Chen XQ, Liu SQ, et al. (2007) Techniques of debris flow prevention in national parks. *Earth Sci Frontiers* 14(6):172-177. [https://doi.org/10.1016/s1872-5791\(08\)60009-3](https://doi.org/10.1016/s1872-5791(08)60009-3)
- Cui P, Liu SQ, Tang BX, et al. (2003) Debris flow prevention pattern in national parks - Taking the world natural heritage Jiuzhaigou as an example. *Sci in China Series E Technological Sci* 46: 1-11. <https://doi.org/10.1360/>
- Cui P, Zou Q, Xiang L-z, et al. (2013) Risk assessment of simultaneous debris flows in mountain townships. *Prog Phys Geog* 37(4): 516-542. <https://doi.org/10.1177/0309133313491445>
- De BS, Poesen J, Gyssels G, et al. (2006) Effects of grass roots on the erodibility of topsoils during concentrated flow. *Geomorphology* 76(1-2): 54-67. <https://doi.org/10.1016/j.geomorph.2005.10.002>
- Dorren LKA, Berger F, le Hir C, et al. (2005a) Mechanisms, effects and management implications of rockfall in forests. *Forest Ecol Manag* 215(1-3): 183-195. <https://doi.org/10.1016/j.foreco.2005.05.012>
- Dorren LKA, Berger F (2005b) Stem breakage of trees and energy dissipation during rockfall impacts. *Tree Physiol* 26: 63-71. <https://doi.org/10.1093/treephys/26.1.63>
- Feistl T, Bebi P, Christen M, et al. (2015) Forest damage and snow avalanche flow regime. *Nat Hazard Earth Sys* 15(6): 1275-1288. <https://doi.org/10.5194/nhess-15-1275-2015>
- Fidej G, Mikoš M, Rugani T, et al. (2015) Assessment of the protective function of forests against debris flows in a gorge of the Slovenian Alps. *iForest* 8(1): 73-81. <https://doi.org/10.3832/ifor0994-007>
- Galia T, Tichavský R, Škarpich V, et al. (2018) Characteristics of large wood in a headwater channel after an extraordinary event: The roles of transport agents and check dams. *Catena* 165: 537-550. <https://doi.org/10.1016/j.catena.2018.03.010>
- Gardiner B, Peltola H, Kellomaki S (2000) Comparison of two models for predicting the critical wind speeds required to damage coniferous trees. *Ecol Model* 129: 1-23.

- [https://doi.org/10.1016/S0304-3800\(00\)00220-9](https://doi.org/10.1016/S0304-3800(00)00220-9)
 Gong XL, Chen KT, Chen XQ, et al. (2020) Characteristics of a debris flow disaster and its mitigation countermeasures in Zechawa Gully, Jiuzhaigou Valley, China. *Water* 12(5).
<https://doi.org/10.3390/w12051256>
- Guthrie RH, Hockin A, Colquhoun L, et al. (2010) An examination of controls on debris flow mobility: evidence from coastal British Columbia. *Geomorphology* 114(4): 601-613.
<https://doi.org/10.1016/j.geomorph.2009.09.021>
- He SM, Liu W, Li XP (2016) Prediction of impact force of debris flows based on distribution and size of particles. *Environ Earth Sci* 75(4): 298.
<https://doi.org/10.1007/s12665-015-5180-2>
- Huebl J, Fiebiger G (2005) Debris-flow mitigation measures. In: Springer Berlin Heidelberg. Praxis.
- Hungr O, Morgan GC, Kellerhals R (1984) Quantitative analysis of debris torrent hazards for design of remedial measures. *Can Geotech J* 21(4): 663-677.
<https://doi.org/10.1139/t84-073>
- Hu KH, Wei FQ, Li Y (2011) Real-time measurement and preliminary analysis of debris-flow impact force at Jiangjia Ravine, China. *Earth Surf Proc Land* 36(9): 1268-1278.
<https://doi.org/10.1002/esp.2155>
- Iverson RM, Denlinger RP (2001) Flow of variably fluidized granular masses across three-dimensional terrain 1. Coulomb mixture theory. *J Geophys Res* 106(10): 537-552.
<https://doi.org/10.1029/2000jb900329>
- Johnson AC, Swanston DN, McGee KE (2000) Landslide initiation, runout, and deposition within clearcuts and old-growth forests of Alaska. *J Am Water Resour As* 36(1): 17-28.
<https://doi.org/10.1111/j.1752-1688.2000.tb04245.x>
- Kwan JSH (2012) Supplementary technical guidance on design of rigid debris-resisting barriers. Geotechnical Engineering Office, Civil Engineering and Development Department, The Government of the Hong Kong Special Administrative Region. https://www.cedd.gov.hk/filemanager/eng/content_486/er270links.pdf
- Li Q, Liu GB, Zhang Z, et al. (2017) Relative contribution of root physical enlacing and biochemical exudates to soil erosion resistance in the Loess soil. *Catena* 153: 61-65.
<https://doi.org/10.1016/j.catena.2017.01.037>
- Liu FZ, Xu Q, Dong XJ, et al. (2017) Design and performance of a novel multi-function debris flow mitigation system in Wenjia Gully, Sichuan. *Landslides* 14(6): 2089-2104.
<https://doi.org/10.1007/s10346-017-0849-0>
- Mitsch WJ (1998) Ecological engineering - the 7-year itch. *Ecol Eng* 10: 119-130.
[https://doi.org/10.1016/S0925-8574\(98\)00009-3](https://doi.org/10.1016/S0925-8574(98)00009-3)
- Moos C, Fehlmann M, Trappmann D, et al. (2018) Integrating the mitigative effect of forests into quantitative rockfall risk analysis – Two case studies in Switzerland. *Int J Disast Risk Re* 32: 55-74.
<https://doi.org/10.1016/j.ijdr.2017.09.036>
- Ng CWW (2017) Atmosphere-plant-soil interactions: theories and mechanisms. *Chin J Geotech Eng* 39(1): 1-46.
<https://doi.org/10.11779/CJGE201701001>
- Olmedo I, Bourrier F, Bertrand D, et al. (2016) Discrete element model of the dynamic response of fresh wood stems to impact. *Eng Struct* 120: 13-22.
<https://doi.org/10.1016/j.engstruct.2016.03.025>
- Olmedo I, Bourrier F, Bertrand D, et al. (2016) Dynamic analysis of wooden rockfall protection structures subjected to impact loading using a discrete element model. *Eur J Environ Civ En.* 24(9): 1430-1449.
<https://doi.org/10.1080/19648189.2018.1472042>
- Peltola H, Kellomäki S (1993) A mechanistic model for calculating windthrow and stem breakage of Scots pines at stand age. *Sliva Fennica* 27(2): 99-111.
<https://doi.org/10.14214/sf.a15665>
- Peltola H, Kellomäki S, Väisänen H, et al. (1999) A mechanistic model for assessing the risk of wind and snow damage to single trees and stands of Scots pine, Norway spruce, and birch. *Can J Forest Res* 29(6): 647-661.
<https://doi.org/10.1139/x99-029>
- Piton G, Recking A (2015) Design of sediment traps with open check dams. II woody debris. *J Hydraul Eng* 142(2): 1-13.
[https://doi.org/10.1061/\(ASCE\)HY.1943-7900.0001049](https://doi.org/10.1061/(ASCE)HY.1943-7900.0001049)
- Pollen, Natasha (2007) Temporal and spatial variability in root reinforcement of streambanks: Accounting for soil shear strength and moisture. *Catena* 69(3): 197-205.
<https://doi.org/10.1016/j.catena.2006.05.004>
- Polster DF, Bio MSRP (2002) Soil bioengineering techniques for riparian restoration. In: Proceedings of the 26th Annual British Columbia Mine Reclamation Symposium, Dawson Creek, BC. pp 230-239
- Poudyal S, Choi CE, Song DR, et al. (2019) Review of the mechanisms of debris-flow impact against barriers. In: Seventh International Conference on Debris-Flow Hazards Mitigation, Golden, Colorado, USA. pp 1027-1034
- Quine CP, Gardiner BA (2007) Understanding how the interaction of wind and trees results in windthrow, stem breakage, and canopy gap formation. *Plant Disturbance Ecology* 13(2): 103-155.
<https://doi.org/10.1016/B978-012088778-1/50006-6>
- Riley B, De LF, Malecot V, et al. (2019) Living concrete: democratizing living walls. *Sci Total Environ* 673: 281-295.
<https://doi.org/10.1016/j.scitotenv.2019.04.065>
- Rossi G, Armanini A (2019) Impact force of a surge of water and sediments mixtures against slit check dams. *Sci Total Environ* 683: 351-359.
<https://doi.org/10.1016/j.scitotenv.2019.05.124>
- Schmid AV, Vogel CS, Liebman E, et al. (2016) Coarse woody debris and the carbon balance of a moderately disturbed forest. *Forest Ecol Manag* 361: 38-45.
<https://doi.org/10.1016/j.foreco.2015.11.001>
- Schmocker L, Weitbrecht V (2013) Driftwood: risk analysis and engineering measures. *J Hydraul Eng* 139(7): 683-695.
[https://doi.org/10.1061/\(asce\)hy.1943-7900.0000728](https://doi.org/10.1061/(asce)hy.1943-7900.0000728)
- Shrestha BB, Nakagawa H, Kawaike K, et al. (2011) Driftwood deposition from debris flows at slit-check dams and fans. *Nat Hazards* 61(2): 577-602.
<https://doi.org/10.1007/s11069-011-9939-9>
- Stokes A, Douglas GB, Fourcaud T, et al. (2014) Ecological mitigation of hillslope instability: ten key issues facing researchers and practitioners. *Plant Soil* 377(1-2): 1-23.
<https://doi.org/10.1007/s11104-014-2044-6>
- Stokes A, Sotir R, Chen W, et al. (2010) Soil bio- and eco-engineering in China: past experience and future priorities. *Ecol Eng* 36(3): 247-257.
<https://doi.org/10.1016/j.ecoleng.2009.07.008>
- Stokes A, Salin F, Kokutse AD, et al. (2005). Mechanical resistance of different tree species to rockfall in the French Alps. *Plant Soil* 278(1): 107-117.
<https://doi.org/10.1007/s11104-005-3899-3>
- Tanaka N, Yagisawa J (2009) Effects of tree characteristics and substrate condition on critical breaking moment of trees due to heavy flooding. *Landsc Ecol Eng* 5(1): 59-70.
<https://doi.org/10.1007/s11355-008-0060-5>
- Tanaka N, Samarakoon MB, Yagisawa J (2011) Effects of root architecture, physical tree characteristics, and soil shear strength on maximum resistive bending moment for overturning *Salix babylonica* and *Juglans ailanthifolia*. *Landsc Ecol Eng* 8(1): 69-79.
<https://doi.org/10.1007/s11355-011-0151-6>
- Thouret JC, Antoine S, Magill C, et al. (2020) Lahars and debris flows: characteristics and impacts. *Earth-Sci Rev* 201: 103003.
<https://doi.org/10.1016/j.earscirev.2019.103003>
- VanDine DF (1996) Debris flow control structures for forest engineering. Res Br, BC Min For, Victoria, BC, Work. Pap. 08/1996.
- Vannoppen W, De Baets S, Keeble J, et al. (2017) How do root and soil characteristics affect the erosion-reducing potential of plant species? *Ecol Eng* 109: 186-195.

- <https://doi.org/10.1016/j.ecoleng.2017.08.001>
Vannoppen W, Poesen J, Peeters P, et al. (2016) Root properties of vegetation communities and their impact on the erosion resistance of river dikes. *Earth Surf Proc Land* 41(14): 2038-2046.
<https://doi.org/10.1002/esp.3970>
- Vannoppen W, Vanmaercke M, De Baets S, et al. (2015) A review of the mechanical effects of plant roots on concentrated flow erosion rates. *Earth-Sci Rev* 150: 666-678.
<https://doi.org/10.1016/j.earscirev.2015.08.011>
- Vagnon F (2019) Design of active debris flow mitigation measures: a comprehensive analysis of existing impact models. *Landslides* 17(2): 313-333.
<https://doi.org/10.1007/s10346-019-01278-5>
- Vergani C, Giadrossich F, Buckley P, et al. (2017) Root reinforcement dynamics of European coppice woodlands and their effect on shallow landslides: A review. *Earth-Sci Rev* 167: 88-102.
<https://doi.org/10.1016/j.earscirev.2017.02.002>
- Wahren A, Schwärzel K, Feger KH (2012) Potentials and limitations of natural flood retention by forested land in headwater catchments: evidence from experimental and model studies. *J Flood Risk Manag* 5(4): 321-335.
<https://doi.org/10.1111/j.1753-318X.2012.01152.x>
- Waldron LJ (1976) The shear resistance of root-permeated homogeneous and stratified soil. *Soil Sci Society of American Journal* 41(5): 843-849.
<https://doi.org/10.2136/sssaj1977.03615995004100050005x>
- Waldron LJ, Dakessian S (1981) Soil reinforcement by roots calculation of increased soil shear resistance from root properties. *Soil Sci* 132(6): 427-435.
<https://doi.org/10.1097/00010694-198112000-00007>
- Wang DP, Chen Z, He SM, et al. (2018) Measuring and estimating the impact pressure of debris flows on bridge piers based on large-scale laboratory experiments. *Landslides* 15(7): 1331-1345.
<https://doi.org/10.1007/s10346-018-0944-x>
- Wang XH, Ma C, Wang YQ, et al. (2020) Effect of root architecture on rainfall threshold for slope stability: variabilities in saturated hydraulic conductivity and strength of root-soil composite. *Landslides* 17(8): 1965-1977.
<https://doi.org/10.1007/s10346-020-01422-6>
- Whelchel AW, Reguero BG, van Wesenbeeck B, et al. (2018) Advancing disaster risk reduction through the integration of science, design, and policy into eco-engineering and several global resource management processes. *Int J Disast Risk Re* 32: 29-41.
<https://doi.org/10.1016/j.ijdrr.2018.02.030>
- Zeng C, Cui P, Su ZM, et al. (2014) Failure modes of reinforced concrete columns of buildings under debris flow impact. *Landslides* 12(3): 561-571.
<https://doi.org/10.1007/s10346-014-0490-0>
- Zhang SC (1993) A comprehensive approach to the observation and prevention of debris flows in China. *Nat Hazards* 7(1): 1-23.
<https://doi.org/10.1007/BF00595676>
- Zhu JL, Shi Y, Fang LQ, et al. (2015) Patterns and determinants of wood physical properties across major tree species in China. *Scientia Sinica Vitae* 45(1): 56-67. (In Chinese)